Effect of Threshold Values Used for Road Segments Detection in SAR Images on Road Network Generation

Şafak Altay Açar
Department of Mechatronics Engineering
Faculty of Technology, Karabük University
Karabük, Turkey

Şafak Bayır
Department of Computer Engineering
Faculty of Engineering, Karabük University
Karabük, Turkey

***Abstract*—In this study, the effect of threshold values used for road segments detection in synthetic aperture radar (SAR) images of road network generation is examined. A three-phase method is applied as follows: image smoothing, road segments detection and irrelevant segments removal. Threshold values used in road segment detection phase are evaluated for four different situations and results are compared. The software is developed to apply and test all situations. Two different synthetic aperture radar images are used in experimental studies.**

***Keywords*—road detection; synthetic aperture radar**

I. Introduction

Since the developments in space technology increase rapidly, more advanced satellites are built. Furthermore, more advanced observing systems are generated to be mounted on these satellites and synthetic aperture radar (SAR) is one of them. SAR can achieve remote imaging effectively for all day (daylight and night) and in all weather conditions [1]. These advantages increase the number of studies on SAR images. Road networks detection has high importance for these studies because knowledge of road networks has strategic importance for national security.

Many academic studies are made on road networks detection in SAR images. Tupin et al. [2] present a study which detects linear features like roads. They use two different line detectors and Markov random field based connection method. Chanussot et al. [3] propose a morphological line detector for road network extraction. To improve the performance, they fuse results of multi-temporal images. Used fusion strategies are tested and compared. Jeon et al. [4] present a genetic algorithm based road detection method. They use perceptual grouping factors to design the fitness function. Dell'Acqua and Gamba [5] develop an algorithm using fuzzy Hough transform to extract roads. Gamba et al. [6] present a study for urban road extraction by utilising proposed algorithm in [5], adaptive directional filtering and perceptual grouping. A new method for a feature based supervised classification is presented by Borghys et al. [7]. They classify SAR images as road, water, forest etc. Chaabouni-Chouayakh and Datcu [8] propose an approach for urban area interpretation. They use mean-shift segmentation, linear structures detector and contextual knowledge to determine roads, buildings etc. A new road centre-point tracking method is presented by Cheng et al. [9]. Local detection and global tracking are applied. He et al. [10] propose a road network grouping algorithm. They use multi-scale geometric analysis of detector responses. Saati et al. [11] present a road centreline extraction research based on a fuzzy algorithm, morphology skeletonisation and snake model. A road detection method is presented by Xiao et al [12]. They use Duda and path operators. Mu et al. [13] propose a new road extraction method based on Otsu method, mathematical morphology and Zernike moments. Cheng et al. [14] present a main road extraction method based on Markov Random Field They accelerate their method by utilising GPU and apply their method to polarimetric SAR images. Jin et al. [15] develop a constant false alarm line detector for polarimetric SAR images. They use Wilks' test statistic which can detect bright and dark features. Jiang et al. [16] propose a road extraction method which uses multi-temporal interferometric SAR covariance. Firstly, they estimate interferometric SAR parameters then detect roads.

The process of road network generation consists of a few sub-processes. Most important ones of them are road segments detection and road segments connecting. The majority of the road network is determined by these two main sub-processes. In this paper, the effect of threshold values used for road segments detection in SAR images on road network generation is examined. Firstly, image smoothing process is applied to SAR images. Then road segments are detected by utilising cross-correlation line detector [2]. Finally, irrelevant segments are removed. Two threshold values are described in road segment detection phase to obtain more accurate results. Threshold values are evaluated for four different situations by using completeness and correctness values.

The rest of the paper is organised as follows: In Section II, image smoothing process is explained. Section III presents road segments detection. Section IV explains the reason of irrelevant segments removing. In Section V, obtained experimental results are evaluated. Section VI presents conclusions and future works.

II. IMAGE SMOOTHING

Noises which are in SAR image have a negative effect on road segment detection; therefore, image smoothing is applied to reduce noises. The 3x3 Gaussian filter is used for this process. The filter is applied to all pixels of SAR image one by one. Pixels' neighbourhood and the filter are shown in Figure 1 and the used equation is defined in (1).

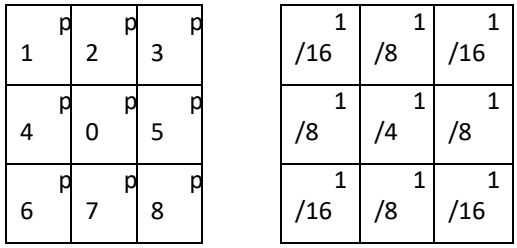

Fig. 1. (a) Pixels' neighbourhood (b) Gaussian filter

$$P_n = \frac{p0}{4} + \frac{(p2+p4+p5+p7)}{8} + \frac{(p1+p3+p6+p8)}{16} \quad (1)$$

In the equation, p0 is relevant pixel's colour value, P_n is the new value of p0 and p1, p2 ,p3 ,p4 ,p5 ,p6 ,p7, p8 are colour values of p0's neighbours.

III. ROAD SEGMENTS DETECTION

After smoothing process, cross-correlation line detector [2] is used to detect road segments. Model of road detector is shown in Figure 2. There is a region 1 in the centre of the model and there are two regions: region 2 and region 3 are placed on the adjacent sides of region 1. Furthermore, relevant pixel p(x,y) is in the centre of region 1.

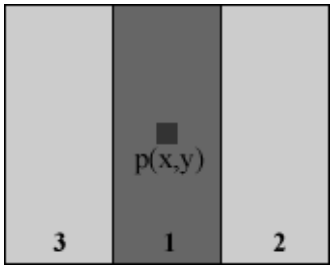

Fig. 2. Model of road detector

Results of adjacent two regions are calculated by utilising (2). In the equation, n_i is the number of pixels in region i, $\bar{c}_{ij}$ is the ratio of mean i and mean j, and γ_i is the ratio of standard deviation and mean [2].

$$p_{ij}^2 = \frac{1}{1+(n_i+n_j)\frac{n_i\gamma_i^2\bar{c}_{ij}^2+n_j\gamma_j^2}{n_i n_j(\bar{c}_{ij}-1)^2}} \quad (2)$$

The result of the detector is calculated by utilising (3). If the p value is higher than predefined threshold p_{min}, p(x,y) is accepted as a part of a road segment. In the experimental studies, we accept p_{min} as 0.4 [2].

$$p = \min(p_{12}, p_{13}) \quad (3)$$

Roads appear as dark structures in SAR images. The detector is applied to only pixels whose colour values are lower than 150 so that pixels which have a high probability of being a part of a road segment, are evaluated. Furthermore, some rules are described. If these rules are not verified, relevant pixel is not accepted as a part of a road segment. Described rules are given in Table 1. In the table, μ_1, μ_2 and μ_3 are mean values of regions and t1 and t2 are threshold values which are evaluated in this study. These threshold values and rules are defined to obtain higher correctness values.

TABLE I. DESCRIBED RULES

No	Rule
1	$\mu_1 < t1$
2	$\mu_2 - \mu_1 > t2$
3	$\mu_3 - \mu_1 > t2$

The detection process is performed for two different road detector models. Differences between these two models are about region widths. In the first one, region 1's width is 3 pixels and other regions' widths are 2 pixels. In the second one, region 1's width is 5 pixels and other regions' widths are 4 pixels. The length of the regions is 11 pixels. Region sizes of models are shown in Figure 3. These region sizes are determined by considering sizes of road structures in SAR images which are used in the experimental studies.

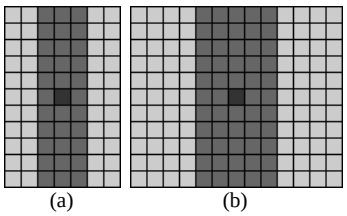

Fig. 3. (a) The first model's region sizes (b) The second model's region sizes

These two models are tested one by one for eight different directions and obtained best value is accepted as a result. Finally, results of models are combined so that process of road segments detection is completed.

IV. IRRELEVANT SEGMENTS REMOVAL

In this process, detected road segments whose sizes are equal or less than 20 pixels are deleted because these segments are too small to be a part of the road network. Steps of this process are as follows:

- An id number is assigned to all pixels which are determined as a part of a road segment in section 3. If there is a pixel with an id number around the relevant pixel, relevant pixel's id number is equalised with this pixel's id number.
- After all relevant pixels have an id number, neighbour segments' id numbers are equalised so that wholeness is realised between segments.
- The size of segments is computed utilising by id numbers. Segments whose sizes are equal or less than 20 pixels are eliminated from road segments.

V. EXPERIMENTAL RESULTS

We developed the software to evaluate four different situations of thresholds values. Two different SAR images

which were acquired by TerraSAR-X are used for experiments. Each of them covers a rural region of 10 km x 10 km. Regions and properties of images are given in Table 2. Images are resized and their sizes are reduced in the ratio of 1/36. After this process, first image's size becomes 2576 x 2299 pixels and second image's size becomes 2553 x 2328 pixels. Sample results of images are shown in Figure 4 and Figure 5 respectively. Red regions denote detected road segments in figures.

TABLE II. REGIONS AND PROPERTIES OF IMAGES

Image	Region	Properties
1	Polatlı (Ankara, Turkey)	Spotlight mode, multi look ground range, HH polarisation, up to 2m resolution
2	Karaman (Turkey)	Spotlight mode, multi look ground range, HH polarisation, up to 2m resolution

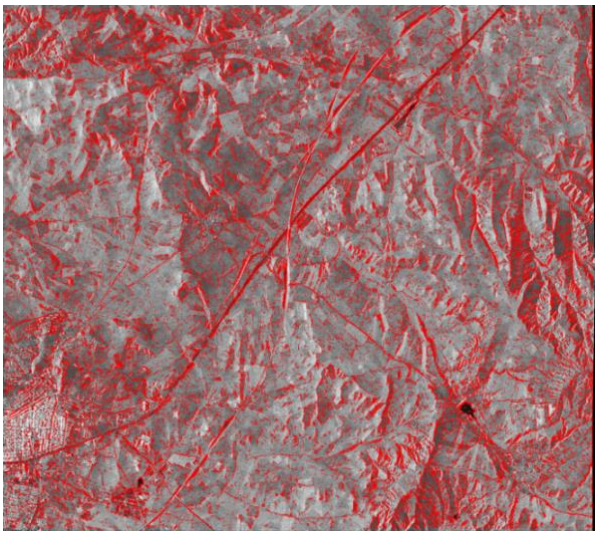

(a)

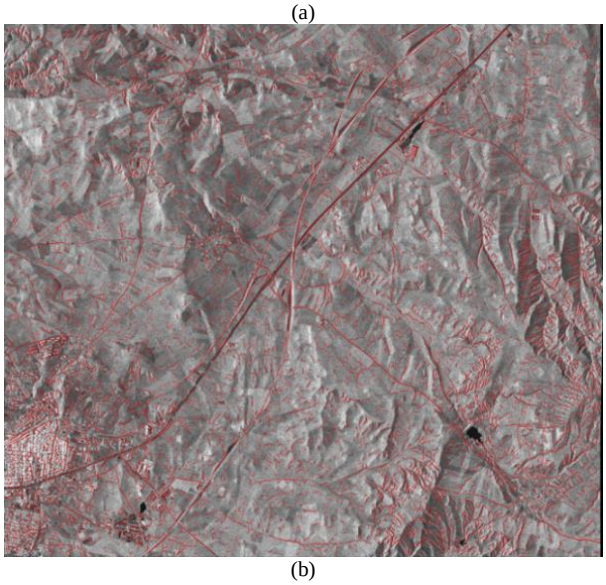

(b)

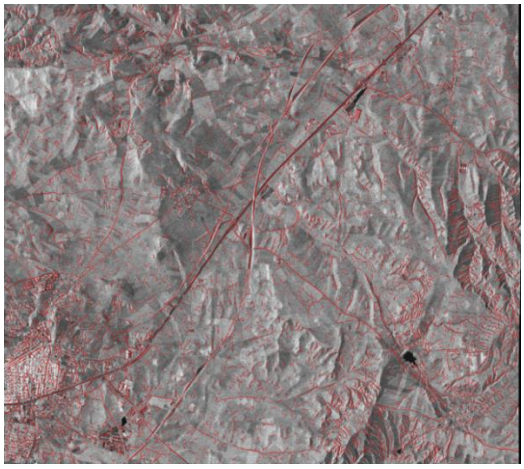

(c)

Fig. 4. First image's results (a) without utilising threshold values (b) threshold values: t1=150, t2=5 (c) threshold values: t1=150, t2=10.

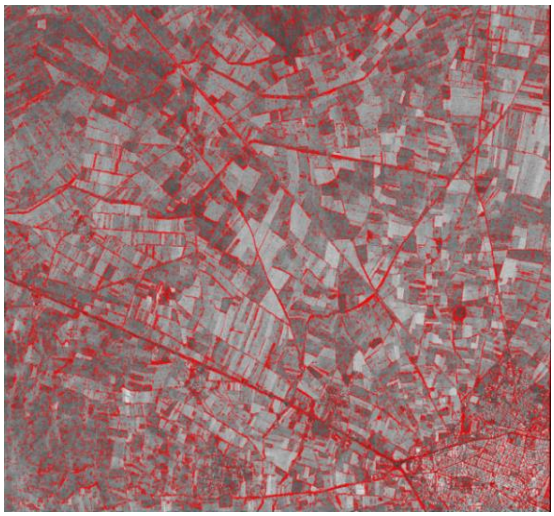

(a)

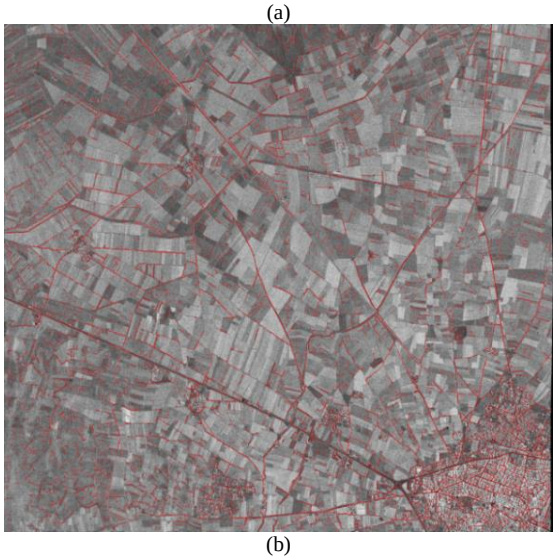

(b)

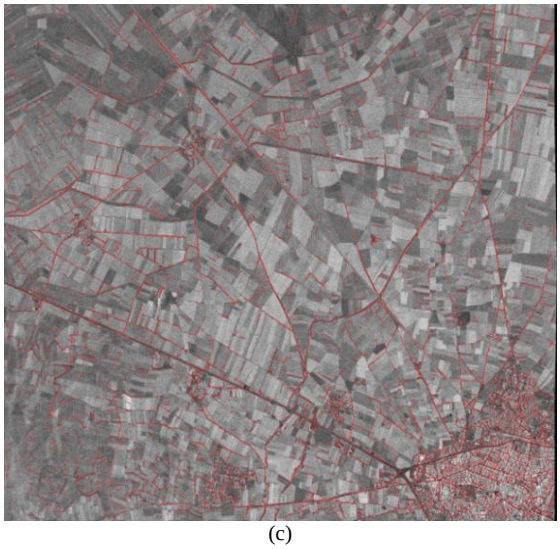

(c)

Fig. 5. Second image's results (a) without utilising threshold values (b) threshold values: t1=120, t2=5 (c) threshold values: t1=120, t2=10.

Detected road segments are compared with real reference roads pixel by pixel. Completeness and correctness values which are defined in (4) and (5) respectively are used for this process. These formulas are similar to the ones described in [17]. Reference pixels are determined by manually. We accept a reference pixel as matched reference pixel if there is a detected pixel in 3x3 pixels around and we accept a detected pixel as matched detected pixel if there is a reference pixel in 3x3 pixels around.

$$\text{comp.} = \frac{\text{number of matched reference pixels x 100}}{\text{number of reference pixels}} \quad (4)$$

$$\text{corr.} = \frac{\text{number of matched detected pixels x 100}}{\text{number of detected pixels}} \quad (5)$$

Firstly completeness and correctness values are calculated without utilising threshold values, then completeness and correctness values are calculated for four different situations: situation 1: (t1=150, t2=5), situation 2: (t1=150, t2=10) situation 3: (t1=120, t2=5) and situation 4: (t1=120, t2=10). According to the obtained results, when threshold values are used, completeness value decreases and correctness value increases. Results of the first image and the second image are given in Table 3 and Table 4 respectively.

TABLE III. RESULTS OF THE FIRST IMAGE

Situation	Decrement of completeness (%)	Increment of correctness (%)
t1=150, t2=5	12.80	135.47
t1=150, t2=10	13.00	166.66
t1=120, t2=5	13.39	202.99
t1=120, t2=10	13.58	248.29

TABLE IV. RESULTS OF THE SECOND IMAGE

Situation	Decrement of completeness (%)	Increment of correctness (%)
t1=150, t2=5	16.79	81.11
t1=150, t2=10	17.31	112.96
t1=120, t2=5	16.85	137.40
t1=120, t2=10	17.37	182.96

When we evaluate the results, assessments occur as follows:

- The increment of correctness is higher than the decrement of completeness in all situations.
- For the first image, decrements of completeness are similar but increments of correctness are different in each situation.
- For the second image, decrements of completeness are similar but increments of correctness are different in each situation.
- The process of road network generation has a few sub-processes such as noise reduction, road segments detection and road segments connecting. Decrements of completeness and increments of correctness affect directly sub-processes which are applied after road segments detection.

VI. CONCLUSION

In this study, the effect of threshold values used for road segments detection in SAR images on road network generation is examined. Two threshold values which are described in road segment detection phase are evaluated for four different situations by using completeness and correctness values. According to results, it is seen that when threshold values are used, completeness value decreases and correctness value increases and increment of correctness is higher than decrement of completeness. These results affect road network generation process directly so we take into consideration this situation when selecting threshold values.

In the future, a whole road network generation method will be developed and each one of sub-processes which compose the method will be evaluated individually.

ACKNOWLEDGMENT

This work was supported by the Scientific Research Coordination Unit of Yıldırım Beyazıt University as a preliminary research project-631.

REFERENCES

[1] A. Moreira, P. Prats-Iraola, M. Younis, G. Krieger, I. Hajnsek, and K. P. Papathanassiou, "A tutorial on synthetic aperture radar," IEEE Geosci. Remote Sensing Mag., vol. 1, no. 1, pp. 6–43, Mar. 2013.

[2] F. Tupin, H. Maitre, J. F. Mangin, J. M. Nicolas, and E. Pechersky, "Detection of linear features in SAR images: application to road network extraction," IEEE Trans. Geosci. Remote Sens., vol. 36, no. 2, pp. 434-453, Mar. 1998.

[3] J. Chanussot, G. Mauris, and P. Lambert, "Fuzzy fusion techniques for linear features detection in multitemporal SAR images," IEEE Trans. Geosci. Remote Sens., vol. 37, no. 3, pp. 1292-1305, May 1999.

[4] B. Jeon, J. Jang, and K. Hong, "Road detection in spaceborne SAR images using a genetic algorithm," IEEE Trans. Geosci. Remote Sens., vol. 40, no. 1, pp. 22-29, Jan. 2002.

[5] F. Dell'Acqua and P. Gamba, "Detection of urban structures in SAR images by robust fuzzy clustering algorithms: the example of street tracking," IEEE Trans. Geosci. Remote Sens., vol. 39, no. 10, pp. 2287-2297, Oct. 2001.

[6] P. Gamba, F. Dell'Acqua, and G. Lisini, "Improving urban road extraction in high-resolution images exploiting directional filtering, perceptual grouping, and simple topological concepts," IEEE Geosci. Remote Sens. Lett., vol. 3, no. 3, pp. 387-391, Jul. 2006.

[7] D. Borghys, Y. Yvinec, C. Perneel, A. Pizurica, and W. Philips, "Supervised feature-based classification of multi-channel SAR images," Pattern Recognition Lett., vol. 27, no. 4, pp. 252-258, Mar. 2006.

[8] H. Chaabouni-Chouayakh and M. Datcu, "Coarse-to-fine approach for urban area interpretation using TerraSAR-X data," IEEE Geosci. Remote Sens. Lett., vol. 7, no. 1, pp. 78-82, Jan. 2010.

[9] J. Cheng, W. Ding, X. Ku, and J. Sun, "Road extraction from high-resolution SAR images via automatic local detecting and human-guided global tracking," Int. Journal of Antennas and Propagation, Nov. 2012.

[10] C. He, Z. Liao, F. Yang, X. Deng, and M. Liao, "Road extraction from SAR imagery based on multiscale geometric analysis of detector responses," IEEE J. Sel. Topics Appl. Earth Observ. Remote Sens., vol. 5, no. 5, pp. 1373-1382, Oct. 2012.

[11] M. Saati, J. Amini, and M. Maboudi, "A method for automatic road extraction of high resolution SAR imagery," Journal of the Indian Society of Remote Sensing, vol. 43, no. 4, pp. 697-707, Dec. 2015.

[12] F. Xiao, Y. Chen, L. Tong, L. He, L. Tan, and B. Wu, "Road detection in high-resolution SAR images using DUDA and path operators," in: IEEE International Geoscience and Remote Sensing Symposium, Beijing, China, Jul. 2016, pp. 1266-1269.

[13] H. Mu, Y. Zhang, H. Li, Y. Guo, and Y. Zhuang, "Road extraction based on ZERNIKE algorithm on SAR images," in: IEEE International Geoscience and Remote Sensing Symposium, Beijing, China, Jul. 2016, pp. 1274-1277.

[14] J. Cheng, W. Ding, X. Zhu, and G. Gao, "GPU-accelerated main road extraction in polarimetric SAR images based on MRF," in: 42nd Annual Conference of the IEEE Industrial Electronics Society, Florence, Italy, Oct. 2016, pp. 928-932.

[15] R. Jin, W. Zhou, J. Yin, and J. Yang, "CFAR line detector for polarimetric SAR images using Wilks' test statistic," IEEE Geosci. Remote Sens. Lett., vol. 13, no. 5, pp. 711-715, May. 2016.

[16] M. Jiang, Z. Miao, P. Gamba, and B. Yong, "Application of multitemporal inSAR coveriance and information fusion to robust road extraction," IEEE Trans. Geosci. Remote Sens., in press.

[17] C. Heipke, H. Mayer, C. Wiedemann, and O. Jamet, "Evaluation of automatic road extraction," Int. Archives of Photogrammetry and Remote Sens., vol. 32, pp. 47-56, 1997.